

Generative Damage Learning for Concrete Aging Detection using Auto-flight Images

T. Yasuno^a, A. Ishii^a, J. Fujii^a, M. Amakata^a, Y. Takahashi^a

^aResearch Institute for Infrastructure Paradigm Shift, Yachiyo Engineering, Co.Ltd, Japan
E-mail: {tk-yasuno,akri-ishii,jn-fujii,amakata,yt-takahashi}@yachiyo-eng.co.jp

Abstract –

In order to health monitoring the state of large-scale infrastructures, image acquisition by autonomous flight drone is efficient for stable angle and high quality image. Supervised learning requires a great deal of dataset consisting images and annotation labels. It takes long time to accumulate images including damaged region of interest (ROI). In recent years, unsupervised deep learning approach such as generative adversarial network (GAN) for anomaly detection algorithms have progressed. When a damaged image is a generator input, it tends to reverse from the damaged state to the health-like state image. Using the distance of distribution between the real damaged image and the generated reverse aging health-like image, it is possible to detect the concrete damage automatically from unsupervised learning. This paper proposes an anomaly detection method using unpaired image-to-image translation mapping from damaged image to reverse aging fake like health condition. Actually, we apply our method to field studies, and we examine the usefulness for health monitoring concrete damages.

Keywords –

Auto-flight monitoring; Aging detection; Image-to-image translation; Concrete infrastructure.

1 Introduction

1.1 Related Works

Starting from a climbing robot for inspection at 2000 [1], there are many researches regarding with autonomous robotics for infrastructure inspection [2]. For example, bridge crack detection [3] using unmanned aerial vehicle (UAV), and so forth. After deep learning revolution 2014 [4], vision-base infrastructure inspection technique have researched using deep learning algorithms [5]. UAV as an autonomous robotics and vision-base deep learning technique has been combined for powerful inspection application [6][7][8][9].

In the field of infrastructure inspection, there are

useful algorithms to detect their damages such as object detection task and semantic segmentation. However, from supervised learning standpoint, the damaged class is rare event and the dataset including that is always imbalance, so the number of rare class images is very small. The more damaged, the less event occurred to collect images. Because of this scarcity of damaged data, it is difficult to improve the accuracy of supervised learning in infrastructure inspection. This is one of hurdle to overcome our underlying problems for infrastructure aging detection for data mining from supervised learning approaches. Instead, this paper proposes an unsupervised deep learning method for aging detection.

Since 2014, the original generative adversarial network (GAN) paper is cited more than 9,000 times to date (July 2019). Starting from GAN's invention in 2014, the field of GAN has been growing exponentially over 360 papers [10]. GANs may be used for many applications, not just fighting breast cancer or generating human faces, but also 62 other medical GAN applications published through the end of July 2018 [11].

Furthermore, unsupervised deep learning approach such as generative adversarial network (GAN) for anomaly detection algorithms have progressed [12]. When a damaged image is a generator input, it tends to reverse from the damaged state to the health-like state image. Using the distance of distribution between the real damaged image and the generated reverse aging health-like image, it is possible to detect the concrete damage automatically from unsupervised learning.

In the field of infrastructure, there are synthetic augmentation researches to mapping from the structure edge label to damaged images such as concrete crack and rebar exposure [13]. Here, the conditional GAN framework pix2pix [14] is one of the most successful using paired images, but the image-to-image, i.e. the one-to-one relation is strong constraint for dataset prepare. Especially, we could not collect the unseen damaged image not yet experienced.

In contrast, the CycleGAN framework is flexible based on unpaired images from domain-A to domain-B. Even if each number of domain image is different, this enable to optimize the end-to-end unsupervised learning.

This paper proposes an anomaly detection method using unpaired image-to-image translation framework CycleGAN, mapping from damaged raw image to reverse aging fake like health condition. Actually, we apply our method to two dam field studies.

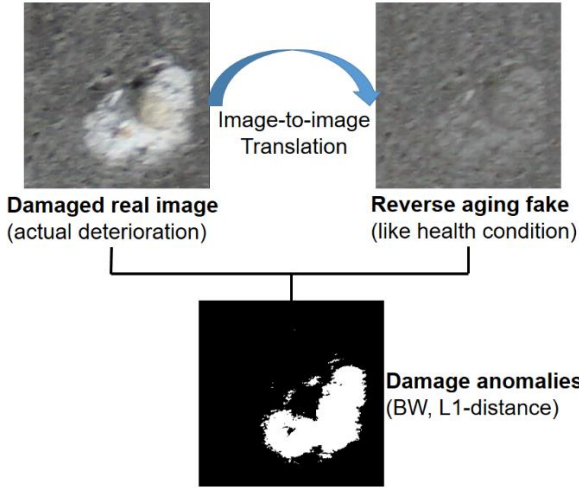


Figure 1. A proposed method using unsupervised generative learning and L1-distance detection.

1.2 Unsupervised Aging Detection Workflow

Figure 1 shows an overview of our method using unsupervised generative learning and L1-distance anomaly detection. This method consists three process.

1. Prepare unpaired images dataset : extract from drone images into unit size images, and divide two subgroup with damaged and health condition.
2. Create generators and discriminators to optimize objective function of CycleGAN networks mapping functions reverse aging (forward) and aging (backward), and cycle consistency.
3. Visualize damage anomalies adapting noise threshold to compute L1-distance between real damaged image and fake output like health condition using the reverse aging generator.

2 Generative Damage Learning Method

2.1 Unpaired Dataset Prepare

First, auto-flight images by drone has 43 images with the pixel size of 6,000 by 3,000 at upper left-side of dam-1 in Kanto region. In this studies, we set the unit size 256 by 256. Without loss of resolution, we resize the original size into 5,888 by 2,816. Because the resized width is 256 multiply 23 and the resized height is 256 multiply 11, without remained surplus. These prepare results in the number of unit images 10,879. Second, we classify two

group of damaged group that includes damaged region of interest (ROI) 4,549 unit images, and health condition image without any damage 6,325 unit images. Furthermore, we classified four group such as 1) health condition without damage (3,852), 2) damaged image (279), 3) blurred (353), 4) repaired region image (69). Thus, we create an unpaired images dataset based on the minimum number 222 that contains domain-D and domain-H. Similarly, regarding with the dam-2 in Tohoku region, auto-flight drone image has the size 6,000 by 4,000, we extracted 12,600 unit images with 256 by 256. This result in another unpaired images dataset with number of 237.

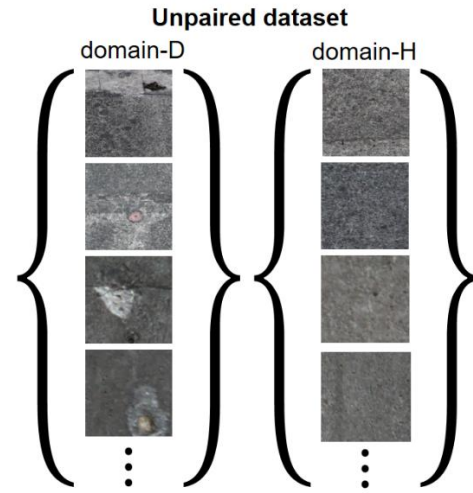


Figure 2. Unpaired images dataset : domain-D (damaged) to domain-H (health condition) translation using CycleGAN framework.

2.2 Damaged-to-normal Image Translation : Reverse Aging via CycleGAN

Figure 3. shows an overview of our applied CycleGAN framework mapping the “reverse aging” (forward) function $R : D \rightarrow H$ and the “aging” (backward) function $F : H \rightarrow D$.

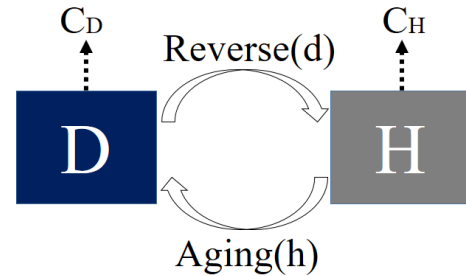


Figure 4. Our applied CycleGAN model mapping functions $R : D \rightarrow H$ and $F : H \rightarrow D$. Discriminator function C_D classifies whether real damaged image or generated fake one, and C_H discriminates whether real health condition image or output fake image.

As Equation (1) shows, for each image d from domain D, the image translation cycle should be able to bring d back to the original damaged image. This is reverse aging (forward) cycle consistency.

$$d \rightarrow R(d) \rightarrow A(R(d)) \approx d. \quad (1)$$

Similarly, As Equation (2) shows, for each image h from domain H, the both translation cycle R and A should be also satisfy aging (backward) cycle consistency.

$$h \rightarrow A(h) \rightarrow R(A(h)) \approx h. \quad (2)$$

Equation (3) stands for full objective function that consists the reverse aging adversarial loss mapping $R : D \rightarrow H$ and discriminator C_H , the aging adversarial loss mapping $F : H \rightarrow D$ and discriminator C_D , and the cycle consistency loss to prevent learned mappings R and A from contradicting each other as follows,

$$\mathcal{L}(R, A, C_D, C_H) = \mathcal{L}_{GAN}(R, C_H, D, H) + \mathcal{L}_{GAN}(A, C_D, D, H) + \lambda \mathcal{L}_{cyc}(R, A) \quad (3)$$

where λ controls relative importance. More detail mathematical representation and network architectures of generator and discriminator are shown as reference [16].

2.3 De-noise Anomaly Detection L1-distance

Using the prediction output (health condition like fake) and the input real damaged image, we propose a anomaly detection based on L1-distance. In order to detect damage anomalies as signal, we have to noise reduce using noise-threshold as a hyper parameter. Furthermore, we try to blob analysis such as area open, dilate image, and clear border. This paper compute the next seven steps image processing as follows:

1. Predict reverse aging output (health-like fake) using trained generator
2. Transform RGB into Grayscale of real and fake
3. Centralize median and set the absolute value
4. Visualize anomalies less than Noise-threshold that is the maximum peak vector exceed median
5. Area open to delete four connected elements less than $0.3 \times \text{Noise-threshold}$
6. Dilate image with structural element “octagon”
7. Clear image border where these are more blight than neighbor with eight connected

3 Applied Results

3.1 Dataset of Auto-flight images

Table 1 shows the case study field of two dams in Japan that we collected images of concrete surface by auto-flight drone. The dam-1 took time 20 years at an earlier deterioration stage. In contrast, the dam-2 is

located in one of snowfall region, and also 62 years passed so that several larger damages have occurred.

Table 1 Dam field profile to data collect by Auto-flight

Profile	Dam-1	Dam-2
Form	Gravity Concrete dam	Arch Concrete dam
Height	156.0m	94.5m
Length of Levee	375.0m	215.0m
Service years	20 years	62 years
Region	Kanto	Tohoku

3.2 Earlier Damage Study : aged 20 years

3.2.1 Training Damaged-to-health Image Reverse Aging Translation

Figure 4 shows the training process of discriminator loss using CycleGAN framework in the field of Kanto region, where the loss values are transformed into the moving average within interval 300 iterations and it plots every 10 iterations skip. This discriminator classify whether the real image in the domain-H (health condition) or fake image. At round 15,000 iterations, the discriminator recognize the generated fake image, but after 40,000 iterations the discriminator often fools the fake image because the generated image approaches to real health condition. It took 17 hours.

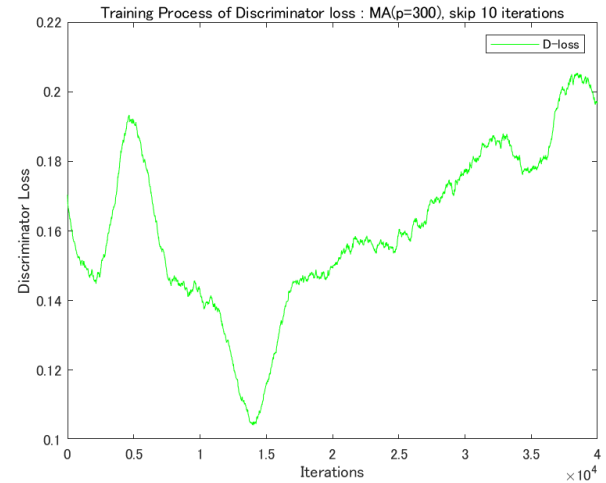


Figure 5. Training process of discriminator loss using CycleGAN framework in the field of Kanto region.

Figure 5 shows the training process of generator loss using CycleGAN framework in the field of Kanto region. This generator transforms from the domain-D (damaged) into the domain-H (health condition). After 40,000 iterations the generator approaches a minimum level.

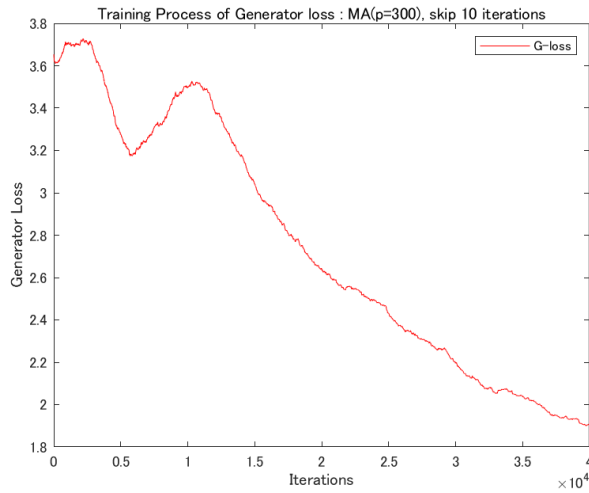


Figure 6. Training process of generator loss using CycleGAN framework in the field of Kanto region.

3.2.2 Anomaly Aging Detection using L1-distance between Raw image and Predicted fake

Figure 6 to 9 shows the dam-1 output results such as damaged image (upper-left) and reverse aging “health condition fake” (upper-right) translated using trained generator mapping from damaged to health. The both real damaged and health-like fake image are subtracted into a gray-scaled L1-distance mask output (bottom). Though small noise remains, our method can detect such as exfoliation, isolated stone, and sand leak. Especially, Figure 9 shows sand leak damage not yet recognized.

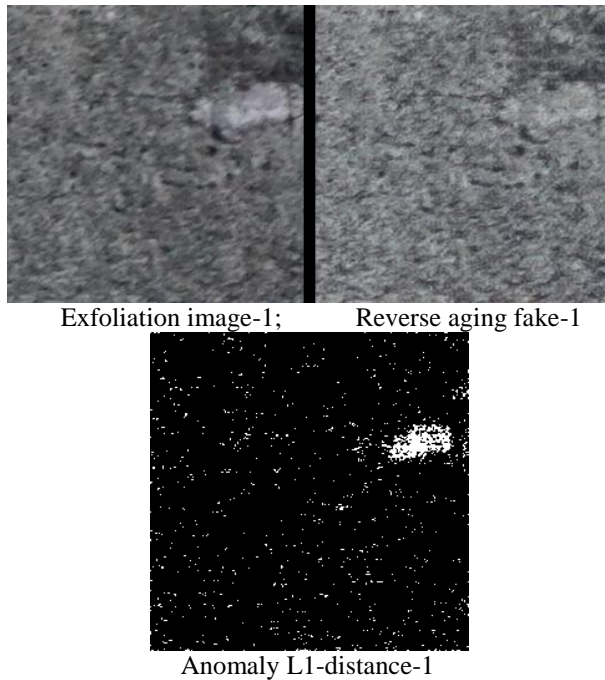


Figure 7. Exfoliation image (upper-left) and reverse aging “health condition fake” (upper-right) translated

using trained generator mapping from damaged to normal image. Gray-scaled L1-distance mask output (bottom).

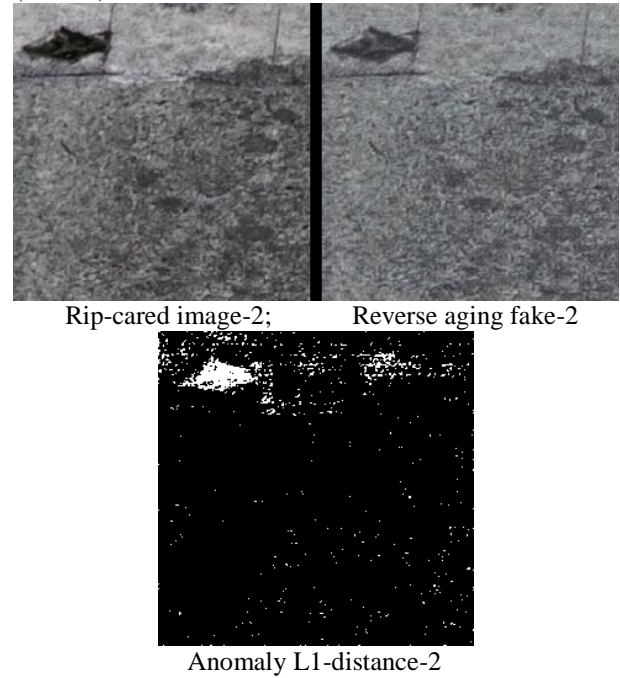


Figure 8. Rip cared image (upper-left) and reverse aging “health condition fake” (upper-right) translated using trained generator mapping from damaged to normal image. Gray-scaled L1-distance mask output (bottom).

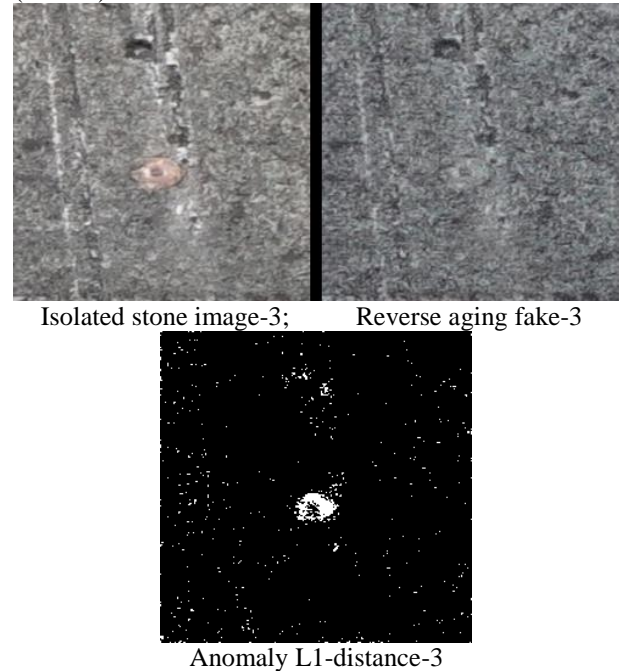


Figure 9. Pre-cause pop-out isolated stone image (upper-left) and reverse aging “health condition fake” (upper-right) translated using trained generator mapping from damaged to normal image. Gray-scaled L1-distance

mask output (bottom).



Figure 10. Sand leak image (upper-left) and reverse aging “health condition fake” (upper-right) translated using trained generator mapping from damaged to normal image. Gray-scaled L1-distance mask output (bottom).

We have a lesson from this dam-1 case 20 years passed. Even if the inspection target class is rare event, using “reverse aging” generator any damage anomalies could be detected. In a dam during 20 years, our method is useful for rip care on the earlier deterioration stage such as sand leak and exfoliation, so as to deny the later progressed damages.

3.3 Cold Damage Study : aged 62 years

3.3.1 Training Damaged-to-health Image Reverse Aging Translation

Figure 10 shows the training process of discriminator loss using CycleGAN framework in the field of Tohoku region, where the loss values are transformed into the moving average within interval 300 iterations and it plots every 10 iterations skip. This discriminator classify whether the real image in the domain-H (health condition) or fake image. After 20,000 iterations, the discriminator repeats to fool the output image because the generated image approaches to real health condition. It took 17 hours.

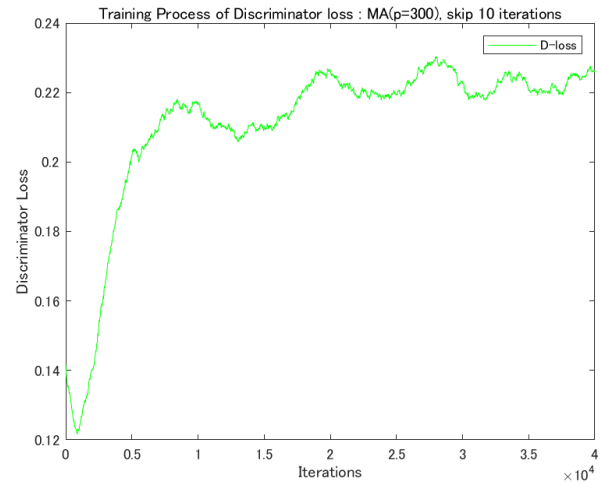


Figure 11. Training process of discriminator loss using CycleGAN framework in the field of Tohoku region.

Figure 11 shows the training process of generator loss using CycleGAN framework in the field of Tohoku region. This generator are mapping from the domain-D (damaged) into the domain-H (health condition). After 30,000 iterations the generator approaches a stable level.

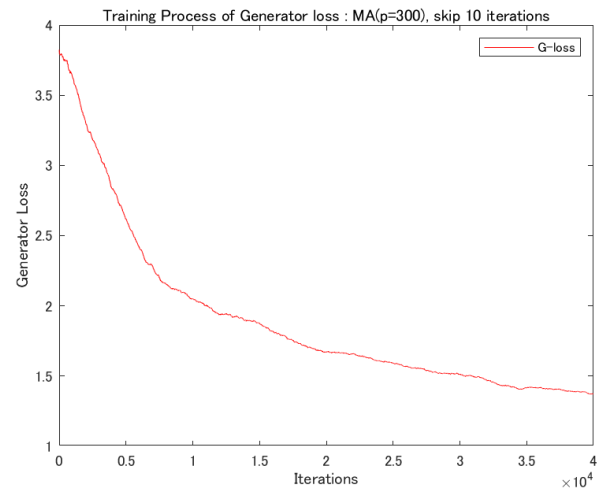


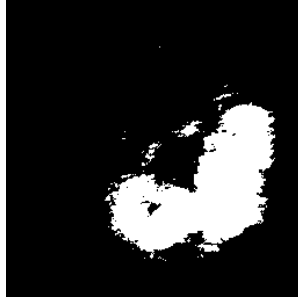
Figure 12. Training process of generator loss using CycleGAN framework in the field of Tohoku region.

3.3.2 Anomaly Aging Detection using L1-distance between Raw image and Predicted fake

Figure 12 to 15 shows the dam-2 detection studies, similar to dam-1, damaged image (upper-left) and reverse aging “health condition fake” (upper-right) translated using trained generator mapping from damaged to health image. The both real damaged and health-like fake image are subtracted into a gray-scaled L1-distance mask output (bottom).



Pop-out crater born image-1; Reverse aging fake-1



Anomaly L1-distance-1

Figure 13. Pop-out crater born image (upper-left) and reverse aging “health condition fake” (upper-right) translated using trained generator mapping from damaged to normal image. Gray-scaled L1-distance mask output (bottom).



Crater-like pop-out image-3; Reverse aging fake-3

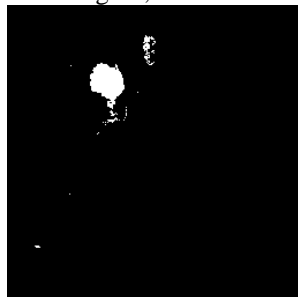


Anomaly L1-distance-3

Figure 15. Crater-like pop-out image (upper-left) and reverse aging “health condition fake” (upper-right) translated using trained generator mapping from damaged to normal image. Gray-scaled L1-distance mask output (bottom).



Soft stone pop-out image-2; Reverse aging fake-2



Anomaly L1-distance-2

Figure 14. Soft stone pop-out image (upper-left) and reverse aging “health condition fake” (upper-right) translated using trained generator mapping from damaged to normal image. Gray-scaled L1-distance mask output (bottom).



Small pop-out image-4; Reverse aging fake-4



Anomaly L1-distance-4

Figure 16. Small pop-out image (upper-left) and reverse aging “health condition fake” (upper-right) translated using trained generator mapping from damaged to normal image. Gray-scaled L1-distance mask output (bottom).

4 Concluding Remarks

4.1 Contributions and Lessons

This paper proposed an anomaly detection method using unpaired image-to-image translation framework CycleGAN, mapping from damaged raw image to reverse aging fake like health condition. Actually, we apply our method to two dam field studies such as one earlier stage aged 20 years, and another one that aged 62 years located in a cold region. The CycleGAN framework is flexible because this input only requires unpaired image dataset such as damage ROI included image and health image without damage. This is a data mining merit instead of the paired image algorithm, for example pix2pix. In addition, our generative unsupervised approach no needs annotation for any classes. After we prepare to extract a unit size images, and divide a damaged group with another health group, we can deep learning end-to-end training a image-to-image translator mapping from damaged domain to health (normal) domain. Even if the inspection target class is rare event, using “reverse aging” generator any damage anomalies could be detected. Experienced from our case studies, in a dam during 20 years our method is useful for rip care on the earlier deterioration stage such as sand leak and exfoliation, so as to deny the later progressed damages.

4.2 Future Works

It needs to optimize a threshold for visualizing the damage anomalies, and for computing the L1-distance between a damaged image and predicted fake like health. This paper did only two case studies of concrete damage, in future we will get further experience different aged periods, different location, different material such as steel, and different infrastructures such as bridge and tunnel. We have to create damage anomalies score using the L1-distance based on the generator of GAN, in addition to another feature matching based on the discriminator of GAN. We try to build another framework that contains a parallel encoder for more efficient damage detection.

[Acknowledgments] We would like to thank S. Kuramoto and T. Fukumoto for providing us generative deep learning MATLAB resources.

References

- [1] Balaguer C., Gimenez A., Pastor J., et al., A climbing autonomous robot for inspection applications in 3D complex environments, *Robotica*, 18, pp287-297, 2000.
- [2] Liu D.K., Dissanayake G., Miro J.V., Waldron K.J., Infrastructure robotics: research challenges and opportunities, 31st International Symposium on Automation and Robotics in Construction and Mining (ISARC), 2014.
- [3] Phung M.D., Dinh T.H., Hoang V.T., et al., Automatic crack detection in built infrastructure using unmanned aerial vehicles, 34th International Symposium on Automation and Robotics in Construction (ISARC), 2017.
- [4] Sejnowski T.J., *The Deep Learning Revolution*, MIT press, 2018.
- [5] Xu S., Wang J., Shou W., Computer vision technique in construction, operation and maintenance phases of civil assets: a critical review, 36th International Symposium on Automation and Robotics in Construction (ISARC), 2019.
- [6] Kucuksubasi, F., Sorguc A.G., Transfer learning-based crack detection by autonomous UAVs, 35th International Symposium on Automation and Robotics in Construction (ISARC), 2018.
- [7] McLaughlin E., Charron N., Narasimhan S., Combining deep learning and robotics for automated concrete delamination assessment, 36th International Symposium on Automation and Robotics in Construction (ISARC), 2019.
- [8] Gopalakrishnan K., Gholami H. et al., Crack damage detection in unmanned aerial vehicle images of civil infrastructure using pre-trained deep learning model, *International Journal for Traffic and Transport Engineering*, 8(1), pp1-14, 2018.
- [9] Yasuno T., Fujii J. Amakata M., Pop-outs segmentation for concrete structure prognosis indices using UAV monitoring and per-pixel prediction, *Proceedings of 12th International Workshop on Structural Health Monitoring* 2019.
- [10] Hindupur A., The GAN zoo, On-line: <https://github.com/hindupuravinash/the-gan-zoo>. Accessed: 15/6/2020.
- [11] Kazemini S. et al., GANs for medical image analysis, <https://arxiv.org/pdf/1809.06222.pdf>.
- [12] Schlegl T., Seebock P., Waldstein S.M. et al., Unsupervised anomaly detection with generative adversarial networks to guide marker discovery, *Proceedings of IPMI* 2017.
- [13] Yasuno T., Nakajima M., Sekiguchi T., Synthetic image augmentation for damage region segmentation using conditional GAN with structure edge, 34th Journal of Society for Artificial Intelligence, 2020.
- [14] Isola, P., Zhu J-Y. et al. : Image-to-image Translation with Conditional Adversarial Network, *CVPR*, 2017.
- [15] Zhu J-Y., Park T., Isola P. et al., Unpaired image-to-image translation using cycle-consistent adversarial networks, arXiv:1703.10593v6, 2018.
- [16] Gonzalez R.C., Woods R.E., *Digital Image*

Processing, 3rd edition, Prentice Hall, 2008.

- [17] Langr J., Bok V., *GANs in Action, Deep Learning with Generative Adversarial Networks*, Manning, 2019.
- [18] Foster D., *Generative Deep Learning : Teaching Machines to Paint, Write, Compose and Play*, O'reilly, 2019.